Low-dose-rate ionizing radiation increases singlet oxygen production by photosensitizers

Xu, Bing; Liu, Juncheng; Eelkema, Rienk; Denkova, Antonia G.

DOI
10.1016/j.xcrp.2025.102976

Publication date
2025

Document Version
Final published version

Published in
Cell Reports Physical Science

Citation (APA)
Xu, B., Liu, J., Eelkema, R., & Denkova, A. G. (2025). Low-dose-rate ionizing radiation increases singlet oxygen production by photosensitizers. *Cell Reports Physical Science*, *6*(12), Article 102976. https://doi.org/10.1016/j.xcrp.2025.102976

Cell Reports
Physical Science

Article

Low-dose-rate ionizing radiation increases singlet oxygen production by photosensitizers

Graphical abstract

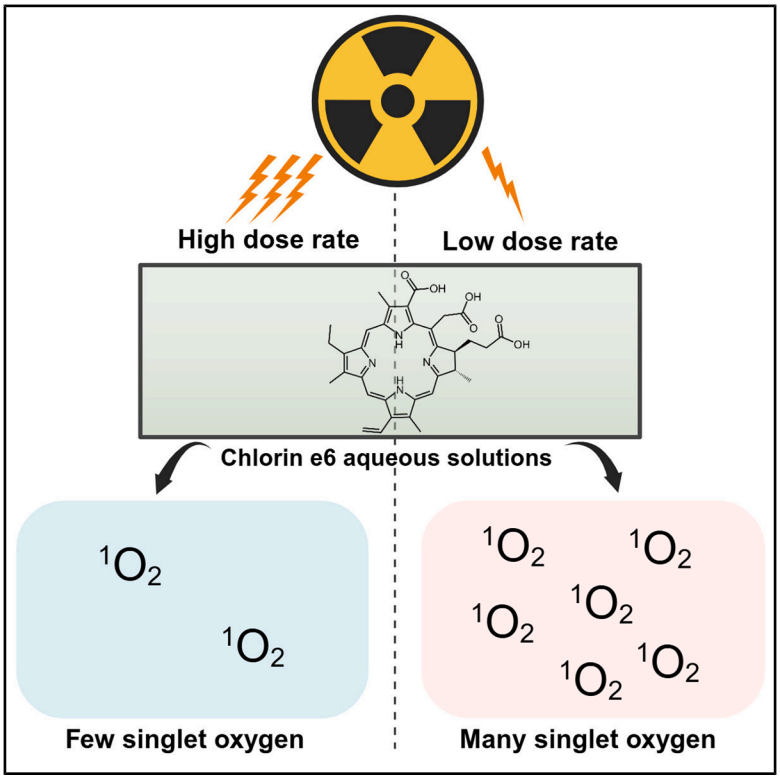

Highlights

- Cerenkov light is not required for singlet oxygen production by Ce6
- A low radiation dose rate enhances singlet oxygen production
- Superoxide anions contribute to singlet oxygen formation

Authors

Bing Xu, Juncheng Liu, Rienk Eelkema, Antonia G. Denkova

Correspondence

r.eelkema@tudelft.nl (R.E.), a.g.denkova@tudelft.nl (A.G.D.)

In brief

Xu et al. reveal that ionizing radiation drives singlet oxygen generation from Ce6 through superoxide anions rather than Cerenkov light, with low dose rates favoring the process by reducing radical recombination.

Xu et al., 2025, Cell Reports Physical Science 6, 102976
December 17, 2025
https://doi.org/10.1016/j.xcrp.2025.102976

CellPress

Cell Reports
Physical Science

CellPress
OPEN ACCESS

Article

Low-dose-rate ionizing radiation increases singlet oxygen production by photosensitizers

Bing Xu,[1,2] Juncheng Liu,[1,2] Rienk Eelkema,[2,*] and Antonia G. Denkova[1,3,*]
[1]Department of Radiation Science and Technology, Delft University of Technology, Mekelweg 15, 2629 JB Delft, the Netherlands
[2]Department of Chemical Engineering, Delft University of Technology, van der Maasweg 9, 2629 HZ Delft, the Netherlands
[3]Lead contact
*Correspondence: r.eelkema@tudelft.nl (R.E.), a.g.denkova@tudelft.nl (A.G.D.)
https://doi.org/10.1016/j.xcrp.2025.102976

SUMMARY

Photosensitizers have significant potential as radiosensitizers in cancer treatment, yet the mechanism of ionizing-radiation-induced singlet oxygen ($^1O_2$) generation remains unclear. Here, we systematically investigated $^1O_2$ production by the photosensitizer Chlorin e6 (Ce6) using the Singlet Oxygen Sensor Green probe and imidazole/*p*-nitroso-*N*,*N*-dimethylaniline detection methods, evaluating the effects of photon energy (X-rays up to 310 kV and ^{60}Co gamma rays at 1.17 and 1.33 MeV), dose, and dose rate. Ce6 produced more $^1O_2$ with increasing photon energy. At 5 Gy, the lowest dose rate (0.005 Gy/min) yielded significantly more $^1O_2$ than higher dose rates (7–0.05 Gy/min). Scavenging experiments identified superoxide anions ($\cdot O_2^-$) as a key intermediate. We propose that, unlike classical triplet-state photosensitization, ionizing radiation induces Ce6 radical cations ($Ce6^{\cdot+}$), which react with radiation-induced $\cdot O_2^-$ to generate $^1O_2$. These findings suggest potential for photosensitizer-radiation combinations in low-dose-rate therapies, although further biological validation and consideration of tumor redox status are required.

INTRODUCTION

Despite the proven effectiveness of radiation therapy (RT) in cancer treatment,[1–5] tumor recurrence remains a significant clinical challenge.[6,7] Radiosensitizers are commonly used to enhance radiation effects in recurrent tumors.[8,9] Although these agents initially achieve tumor growth delay, their systemic toxicity ultimately limits improvements in overall survival.[10] Photosensitizers (PSs), which are traditionally used in photodynamic therapy (PDT) to generate cytotoxic singlet oxygen ($^1O_2$) and other reactive oxygen species (ROS) upon light activation,[11] have emerged as promising alternatives, offering remarkable potential to enhance radiation effects with minimal toxicity. Early PSs, such as hematoporphyrin and Photofrin, achieved clinical success in inducing tumor remission when combined with RT,[12–16] having as its only side effect prolonged photosensitivity persisting for months after treatment.[17] Recently, 5-aminolevulinic acid (5-ALA) has gained a lot of attention as a precursor that converts intracellularly into protoporphyrin IX (PpIX), the latter selectively accumulating in tumor tissues due to altered heme biosynthesis,[18] thereby reducing systemic phototoxicity and enhancing radiotherapy outcomes. Preclinical studies have established the feasibility of 5-ALA as a radiosensitizer,[19–22] prompting its clinical translation, with ongoing clinical trials focused on evaluating the maximum tolerated dose of 5-ALA.[23] However, the fundamental interaction mechanism between ionizing radiation and photosensitizers that is responsible for these results has received limited attention, preventing optimization of the therapeutic outcomes.

Photosensitizers are typically activated by light photons, which excite them to a triplet state and lead to the generation of $^1O_2$ and ROS.[24] However, there is some evidence suggesting that this classical mechanism may not apply under ionizing radiation. For instance, research by Takahashi and Misawa suggest that under X-ray radiation, PpIX may generate ROS through a mechanism involving the transfer of radical energies from primary radicals such as hydroxyl radicals (·OH), hydrogen radicals (·H), and hydrated electrons (e_{aq}^-), as well as secondary electrons, to PpIX.[25] Similarly, Schaffer et al. observed comparable biological effects of Photofrin at radiation doses of 5 Gy and 15 Gy, further suggesting that the observed results may not be caused by direct interaction of photosensitizers with radiation,[13] such as photon excitation. Some cell studies performed to understand the observed cytotoxicity when using 5-ALA suggest that the effects are mediated by enhanced intracellular ROS production, especially superoxide anions ($\cdot O_2^-$), from mitochondrial dysfunction.[26,27] This mechanism is particularly relevant to 5-ALA due to PpIX accumulation in mitochondria. However, direct evidence linking the dysfunction of mitochondria during irradiation in the presence of PSs is still lacking. In addition, most existing studies have focused on factors such as photon energy or radiation type (photons vs. particles), while the potential influence of dose rate has often been overlooked. Moreover, the diversity of experimental conditions, including cell types, has led to conflicting or non-comparable results. For instance, photons having both keV and MeV energies appear to be able to activate PSs,[19,20,22] while some studies attribute the effect to Cerenkov radiation that only occurs at

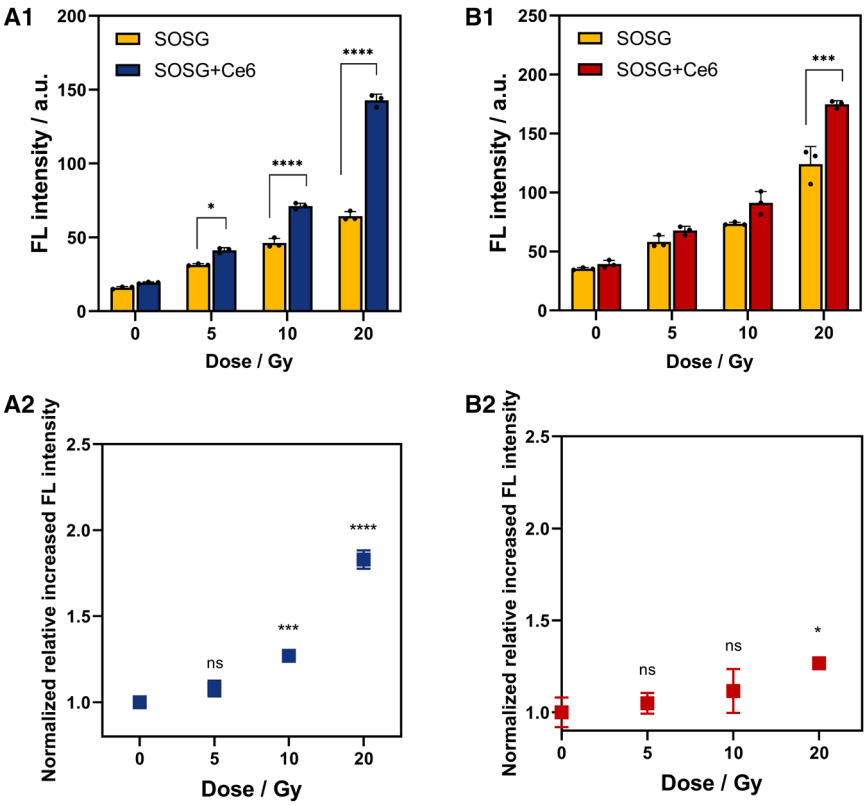

Figure 1. Higher-energy gamma-ray radiation enhances SOSG fluorescence in the presence of Ce6 compared with X-ray radiation

The direct fluorescence intensity values of SOSG in samples after exposure to (A1) a ^{60}Co source emitting gamma energy of 1.17 and 1.33 MeV at a dose rate of 6.2 Gy/min and (B1) X-rays with a dose rate of 7 Gy/min (310 kV, 12 mA). (A2) and (B2) represent the normalized relative increase of fluorescence intensity of SOSG in Ce6-containing samples compared to the control groups, corresponding to (A1) and (B1), respectively, as calculated using Equations 4 and 5 (see methods). All data are presented as mean ± SD and were analyzed by two-way ANOVA (A1 and B1) or one-way ANOVA (A2 and B2). *$p < 0.05$, ***$p < 0.0005$, ****$p < 0.0001$; $n = 3$. [Ce6] = 5 μM; [SOSG] = 5 μM.

high photon energies,[28,29] as its emission spectrum overlaps with PS absorption wavelengths.[30]

In this study, we have systematically investigated the activation of photosensitizers by X-rays and gamma rays, addressing key factors that may influence their behavior. Specifically, this study considers the energy of photons (below and above the threshold of Cerenkov light production), the effect of dose rate, and the role of free radicals in pure water. Given that $^1O_2$ is recognized as one of the most cytotoxic species,[31] we primarily focus on its formation during ionizing radiation. The photosensitizer Chlorin e6 (Ce6) was chosen, due to its better water solubility compared to most porphyrins and previous findings indicating its activation under ionizing radiation.[32]

RESULTS

Higher photon energy enhances singlet oxygen production at comparable dose rates

This section aims to investigate the role of radiation energy in activating Ce6, taking also into account possible Cerenkov light generation. To address this, two external radiation sources—X-rays and gamma rays—were employed to deliver photons of different energies. The energy of the X-rays used was 310 kV, which will not produce Cerenkov light, while the energy of the gamma rays delivered by a ^{60}Co source are well above the limit of Cerenkov light generation (i.e., 1.17 and 1.33 MeV). The activation of Ce6 was evaluated by measuring the formation of singlet oxygen ($^1O_2$) according to changes in fluorescence intensity (FL intensity) of the Singlet Oxygen Sensor Green (SOSG) probe. Samples containing Milli-Q (MQ) water with the same concentration of SOSG were used as a control group to account for any potential interaction of SOSG itself with ionizing radiation.

Figure 1 shows the FL intensity of SOSG in samples with or without Ce6 exposed to gamma- or X-ray radiation. After exposure to gamma rays at a dose rate of 6.2 Gy/min (Figure 1A1), a significant increase in FL intensity was observed beyond 5 Gy in the Ce6 group compared to the control group, with a more pronounced enhancement at 10 and 20 Gy. To ensure comparable conditions with gamma-ray exposure, the dose rate of X-rays was set to 7 Gy/min (Figure 1B1), using a voltage of 310 kV and a current of 12 mA. A modest increase in FL intensity was noted at 20 Gy in the Ce6 group compared to controls.

We noticed that the SOSG fluorescence also increased with radiation dose in the absence of Ce6 (Figure S1). This radiation-induced response was further confirmed by the fluorescence spectra (Figure S2A) and has been previously reported by Liu et al.,[32] who showed that the fluorescence signal was influenced by ·OH produced during ionizing radiation. Consistently, the UV spectral analysis revealed decreased absorption at 257 nm (Figure S2B), suggesting ·OH-mediated modification of SOSG's anthracene moiety,[33] which could disrupt its fluorescence-quenching mechanism.

To properly assess the ability of Ce6 to generate $^1O_2$ compared to SOSG solutions alone, additional calculations were performed. First, the relative increase in the Ce6 group at each dose compared to the control group was calculated using Equation 4 (see methods). These values were then normalized to the relative FL intensity at 0 Gy according to Equation 5 (see methods) to further isolate the effect of Ce6 from the baseline fluorescence differences at 0 Gy.

Figures 1A2 and 1B2 present the data processed from Figures 1A1 and B1 based on the described corrections. After

Table 1. Settings used for delivering 5 Gy by X-ray radiation

Energy	310 kV, 12 mA	240 kV, 15 mA	240 kV, 1 mA	240 kV, 1 mA	240 kV, 0.7 mA	240 kV, 1 mA
Dose rate (Gy/min)	7	3	0.195	0.05	0.034	0.005
Distance (cm)	11	21	21	46	46	150
Irradiation time	40 s	1 min 42 s	25 min 38 s	100 min	147 min	16 h 30 min

normalization, an increase that was initially observed for a dose below 5 Gy under gamma-ray radiation (Figure 1A1) was no longer evident (Figure 1A2). The normalized relative FL intensities for 5 Gy, 10 Gy, and 20 Gy were 1.080 ± 0.046, 1.270 ± 0.036, and 1.829 ± 0.054, respectively. No significant increase was observed at 5 Gy in the Ce6 group, while significant differences in FL intensity were observed at 10 Gy ($p < 0.0005$) and 20 Gy ($p < 0.0001$) compared to non-irradiated samples. For the samples irradiated with X-rays at a dose rate of 7 Gy/min, the normalized FL intensity values were 1.049 ± 0.055, 1.116 ± 0.119, and 1.266 ± 0.023 for 5 Gy, 10 Gy, and 20 Gy, respectively. A significant enhancement was observed at 20 Gy ($p < 0.05$) (Figure 1B2).

The lowest dose rate, 0.005 Gy/min, leads to the highest singlet oxygen production

The findings from the previous section demonstrate that Cerenkov light was not essential for activating Ce6, as $^1O_2$ was also detected when using X-rays with energy below the Cerenkov threshold. Building on these results, this section investigates the effect of dose rate on $^1O_2$ production, a factor that differs significantly between external and internal radiation.[34] Given the unpredictable dose rates inherent to radionuclide therapy, the lowest dose rate used here was 0.005 Gy/min, comparable to that used in low-dose-rate brachytherapy.[35] X-rays with an energy of 240 kV were used to avoid Cerenkov light formation, and the voltage-to-current ratio of the X-ray source was adjusted to achieve the desired dose rates, as detailed in Table 1.

Figure 2 shows the measurement of $^1O_2$ using the SOSG probe and the imidazole/*p*-nitroso-*N*,*N*-dimethylaniline (Imd/RNO) method. In Figure 2A, the FL intensity of the SOSG in samples following 5 Gy of X-ray radiation at various dose rates are depicted. After normalization (Figure 2B), the greatest enhancement in FL intensity in the presence of Ce6 was observed at 0.005 Gy/min, with a normalized relative increase of 2.505 ± 0.026 compared to non-irradiated samples. The corresponding values for dose rates of 7, 3, 0.2, and 0.05 Gy/min were 1.361 ± 0.108, 1.416 ± 0.131, 1.413 ± 0.115, and 1.580 ± 0.024, respectively. Statistical analysis showed that the normalized relative FL intensity at 0.005 Gy/min was significantly higher than those at higher dose rates ($p < 0.0001$). In contrast, the normalized relative FL intensities at dose rates of 7, 3, 0.2, and 0.05 Gy/min did not differ significantly from each other; however, a slight increase was observed compared to non-irradiated groups. The different results at 5 Gy observed in our study between Figures 1B1 and 2B at 7 Gy/min may be due to variations in SOSG batches, as differences in solubility and sensitivity to $^1O_2$ could lead to the discrepancies in measured intensities.

To confirm the results obtained using SOSG, we used a second method for detecting $^1O_2$, known as the Imd/RNO method. This method showed effective detection of $^1O_2$ generation (Figure S3A), which was completely inhibited by the $^1O_2$ quencher NaN_3 (Figure S3B). In our experiments, the absorption of RNO was measured before and after the irradiation. The change in absorption ($\Delta A = A_{\text{before radiation}} - A_{\text{after radiation}}$) was used to evaluate the ability of Ce6 to generate $^1O_2$. When applying this method under ionizing radiation, it should be noted that RNO also quenches ·OH generated during water radiolysis,[36] which can lead to the decrease of RNO absorption and interfere with the detection of $^1O_2$. To minimize this effect, ethanol was added as a strong ·OH scavenger to protect RNO.[37] At a radiation dose of 70 Gy, a clear decrease in RNO absorption was observed in the RNO solution, but this effect was eliminated in the presence of 0.01% ethanol, confirming its protective role (Figure S4A). In all subsequent X-ray irradiation experiments, 0.01% ethanol was present unless otherwise specified.

Figure 2C shows the absorption change of RNO in the presence of Ce6 before and after X-ray exposure. At a dose of 5 Gy delivered at a dose rate of 0.005 Gy/min, RNO absorption decreased significantly by 0.126 ± 0.013 ($p < 0.0001$ compared to other groups). In contrast, no significant decrease in RNO absorption was observed when samples were irradiated at higher dose rates (7, 3, 0.2, and 0.034 Gy/min). A similar decrease at 0.005 Gy/min was also observed with Ce6 in the absence of ethanol, whereas the control groups (Ce6 + RNO, L-histidine + RNO, and RNO), with or without ethanol, showed only minor changes (Figure S4B). For higher dose rates, the control groups (Ce6 + RNO, L-histidine + RNO, and RNO) exhibited negligible changes in RNO absorption (Figure S4C).

Superoxide anions are involved in singlet oxygen formation

Research has suggested that free radicals from water radiolysis may play a role in the activation process of photosensitizers.[13,25] Our experimental results showed that when using the Imd/RNO method, the addition of ethanol had no effect on the formation of $^1O_2$ by Ce6 (Figure S4B), indicating that ·OH were not involved in the formation process. To further explore the mechanism under ionizing radiation, we evaluated the role of free radicals, particularly superoxide anions ($\cdot O_2^-$), which have been shown to be influenced by dose rate due to possible radical-radical recombination.[38] This was achieved by introducing an $\cdot O_2^-$ scavenger, superoxide dismutase (SOD), during radiation exposure.

As shown in Figure 3A, the addition of 1 μg/mL SOD did not affect the intrinsic fluorescence of SOSG without X-ray exposure, nor did it alter SOSG behavior after light exposure (Figure S5A). In the absence of SOD, exposure to 5 Gy of X-rays at 0.005 Gy/min resulted in an increase in FL intensity of SOSG in the Ce6 group compared to the control group, consistent with earlier findings. However, this increase was eliminated

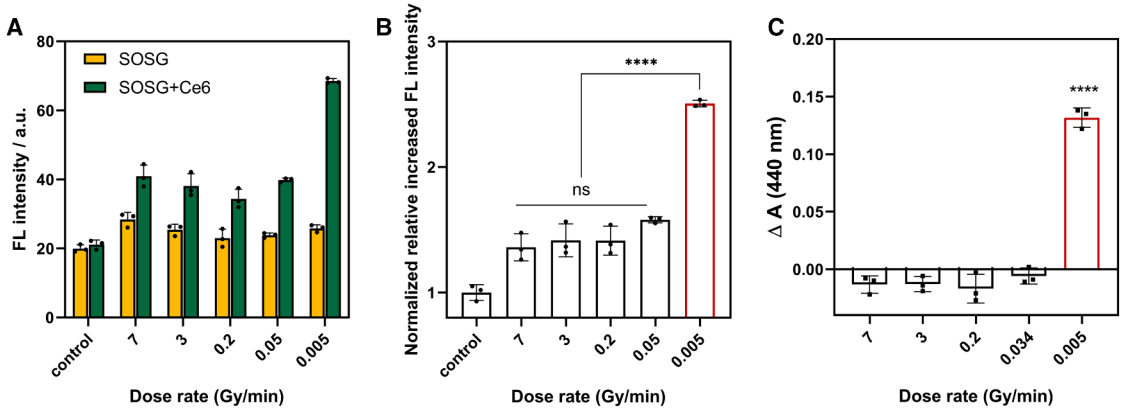

Figure 2. Low-dose-rate radiation enhances SOSG fluorescence and RNO bleaching in the presence of Ce6

(A) Fluorescence intensity of SOSG in samples with or without Ce6. [Ce6] = 5 μM; [SOSG] = 5 μM.

(B) Normalized relative increase in fluorescence intensity based on data derived from (A).

(C) Absorption difference of RNO in the presence of Ce6 before and after X-ray irradiation. Samples contained 40 μM Ce6, 50 μM RNO, and 10 mM L-histidine; Δ*A* denotes the difference between the absorption of RNO before and after irradiation; pH was set to 7.4 using phosphate buffer (PB).

All data are presented as mean ± SD and were analyzed by one-way ANOVA (B and C). ****$p < 0.0001$; ns, not significant; $n = 3$.

with the addition of SOD, as indicated by the lack of significant difference between the Ce6 group and the control group with SOD after irradiation. Similarly, the addition of SOD did not affect the decrease of RNO absorption in presence of Ce6 under sunlight exposure (Figure S5B). In Figure 3B, a significant decrease of RNO absorption was observed in the Ce6 group without SOD when compared to the control group without Ce6 after exposure to 5 Gy at a dose rate of 0.005 Gy/min. However, this decrease in RNO absorption in the presence of Ce6 was also eliminated by the addition SOD, showing a significant difference when compared to the Ce6 group without SOD. Furthermore, in the presence of SOD, no significant difference was observed between the Ce6 group and the control group.

The effect of SOD on the FL intensity of SOSG in the presence of Ce6 was also studied under gamma-ray exposure. Figure 3C shows that after 20 Gy of gamma-ray radiation, the FL intensity of SOSG in the presence of Ce6 was significantly higher than that of the control group. However, after adding SOD, this increase disappeared, and no difference in the FL intensity of SOSG was observed between the Ce6 group and control group. Notably, SOSG itself still had higher FL intensity after 20 Gy radiation compared to 0 Gy regardless of the addition of SOD.

The UV absorption of SOSG molecules both before and after irradiation in the presence of SOD was measured to check whether SOD would structurally influence the SOSG molecule (Figure S5C). The UV spectrum shows that the addition of SOD

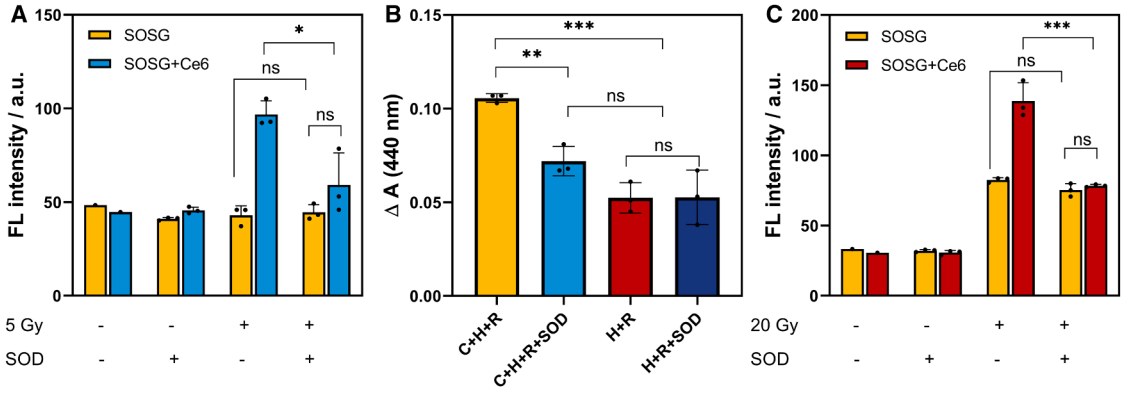

Figure 3. Addition of SOD eliminates the increase in SOSG fluorescence and RNO bleaching in the presence of Ce6

(A and B) Samples were exposed to 5 Gy of X-rays (240 kV, 1 mA; dose rate = 0.005 Gy/min). (A) Fluorescence change of SOSG. [Ce6] = 5 μM; [SOSG] = 5 μM; [SOD] = 1 μg/mL. (B) Change in RNO absorption. C + H + R samples contained 40 μM Ce6, 10 mM L-histidine, and 50 μM RNO; C + H + R + SOD samples contained 40 μM Ce6, 10 mM L-histidine, 50 μM RNO, and 1 μg/mL SOD; H + R samples contained 10 mM L-histidine and 50 μM RNO; H + R + SOD samples contained 10 mM L-histidine, 50 μM RNO, and 1 μg/mL SOD; Δ*A* denotes the difference between the absorption of RNO before and after irradiation; pH was set to 7.4 using PB.

(C) Fluorescence of SOSG after exposure to 20 Gy of gamma-ray radiation (1.17 and 1.33 MeV) at a dose rate of 6.2 Gy/min. [Ce6] = 5 μM; [SOSG] = 5 μM; [SOD] = 1 μg/mL.

All data are presented as mean ± SD and were analyzed by one-way ANOVA. *$p < 0.05$, **$p < 0.01$, ***$p \leq 0.0005$; $n = 3$.

did not affect the molecular structure of SOSG, even after irradiation, as no noticeable decrease in SOSG absorption was observed.

DISCUSSION

In this study, we systematically investigated $^1O_2$ generation by Ce6 under ionizing radiation, focusing on key factors such as radiation energy (below or above the threshold of generating Cerenkov light in water), dose rate, and the effects of free radicals. We primarily evaluated $^1O_2$ formation using the SOSG probe during irradiation by measuring the increase in FL intensity at an emission wavelength of 528 nm. Additionally, we used the Imd/RNO method as a complementary approach to validate the obtained results.

X-rays with energy up to 310 kV and gamma rays with energy of 1.17 and 1.33 MeV can both activate Ce6 to produce $^1O_2$, with increasing doses leading to more $^1O_2$ production (Figure 1). Gamma rays appeared to be more efficient than X-rays in activating Ce6 when compared at similar dose rates, achieving higher $^1O_2$ production at a lower dose. This enhanced response was specific to Ce6, as the SOSG controls showed comparable behavior under both X-ray and gamma-ray radiation (Figure S1A). While gamma rays generated more $^1O_2$, several observations suggest that this enhanced production is not driven by Cerenkov radiation. First, at the energy levels used in this study, gamma rays produced minimal Cerenkov radiation.[39] Second, X-ray radiation successfully generated $^1O_2$ (Figures 1B1 and S6), despite the absence of Cerenkov light (Figure S7). These observations suggest that the difference in $^1O_2$ production between gamma rays and X-rays is likely driven by their energy and related interaction mechanism.

The relationship between dose rate and $^1O_2$ production exhibits a distinct pattern, where dose rates ranging from 0.05 Gy/min to 7 Gy/min showed minimal impact; a significant increase was observed at the much lower dose rate, i.e., 0.005 Gy/min (Figures 2A and 2B). To address the potential interference from SOSG, this observation was further validated using the Imd/RNO method, which further confirmed that the lowest dose rate (0.005 Gy/min) led to a substantial increase in $^1O_2$ production (Figure 2C). Furthermore, the decrease in RNO absorption was consistent for samples with and without ethanol, confirming that the reduction in RNO can be attributed to the formation of $^1O_2$ and not of ·OH (Figure S4B). To the best of our knowledge, this study is the first to demonstrate that radiation dose rate affects the production of $^1O_2$ by photosensitizers, as demonstrated here by Ce6.

There are no reports investigating similar effects in other types of photosensitizers. In principle, photosensitizers such as Ce6 are activated by absorbing an incident photon with energy of approximately 1.14 eV to ultimately form a triplet state,[40] which can subsequently transfer energy to $^3O_2$ and form $^1O_2$. However, it is very unlikely for ionizing radiation to follow this activation pathway, as energy of ionizing radiation far exceeds 1.14 eV. Instead, this activation may occur in subsequent steps, where the energy deposited by ionizing radiation into the surrounding medium (e.g., water) triggers subsequent indirect processes that ultimately lead to the production of $^1O_2$ by Ce6.

The energy deposition of ionizing radiation in water is categorized into three main stages: the physical stage ($\sim10^{-15}$ s), the physicochemical stage (10^{-15} to $\sim10^{-12}$ s), and the chemical stage (10^{-12} to $\sim10^{-6}$ s). During the initial physical stage, the primary ionizations produce secondary electrons through excitation and ionization of surrounding molecules. These secondary electrons undergo cascading energy loss, eventually generating low-energy electrons that can no longer induce molecular excitation or ionization.[41] One could expect that these low-energy electrons having energy above 1.14 eV could transfer energy to Ce6 molecules, resulting in the triplet state of Ce6 and in turn producing $^1O_2$, which might explain the dose-dependent manner of the increased FL intensity of SOSG with Ce6 (Figure 1), as the production of secondary electrons is dose dependent.

The energy deposition of low-energy electrons predominantly depends on the initial radiation energy.[41,42] If these electrons were solely responsible for Ce6 activation, $^1O_2$ production should remain consistent at a given dose regardless of the dose rate. However, our observations at 5 Gy across different dose rates showed dose-rate-related variations in $^1O_2$ production despite nearly identical X-ray energy spectra (Figure S7), suggesting the involvement of processes beyond the physical stage. While the excited H_2O^* molecules (with energy ~1.3 eV above the first ionization potential[42]) could potentially transfer energy to Ce6, their short lifetime (~0.8 ps[43]) and low yield[42] make their contribution negligible.

Dissolved molecular oxygen plays a crucial role as a precursor to $^1O_2$. During exposure to ionizing radiation, a continuous consumption of O_2 occurs through the following reactions[44]:

$$e_{aq}^- + O_2 \leftrightarrows \cdot O_2^-,$$

$$H^\cdot + O_2 \leftrightarrows HO_2^\cdot$$

At lower dose rates, two factors could potentially enhance the energy-transfer process between Ce6 and oxygen: the slower O_2 consumption rate compared to high dose rates, which allows Ce6 molecules to be surrounded by more O_2; and the longer irradiation time, which enables more efficient O_2 replenishment. This could theoretically provide more opportunities for Ce6 to transfer energy to surrounding oxygen. However, given that the dissolved O_2 concentration in water under normal atmospheric pressure (~250 μM) is sufficiently high, a 5 Gy dose would not significantly deplete it.[45] Therefore, O_2 availability is unlikely to be a limiting factor in Ce6 activation. Rather, free radicals and molecular products generated during irradiation appear to be more probable drivers of Ce6 activation and subsequent $^1O_2$ production.

Recent studies have shown that the yield of free radicals, such as ·OH and e_{aq}^-, varied with dose rate, possibly due to the complicated intra-track radical-radical recombination.[38,46] The Imd/RNO results (Figure 2C) clearly indicated that ·OH was not involved in the generation of $^1O_2$ by Ce6 because upon measurement performed in the presence of ethanol, a known quencher of ·OH, a substantial amount of $^1O_2$ was still formed at a dose rate of 0.005 Gy/min.

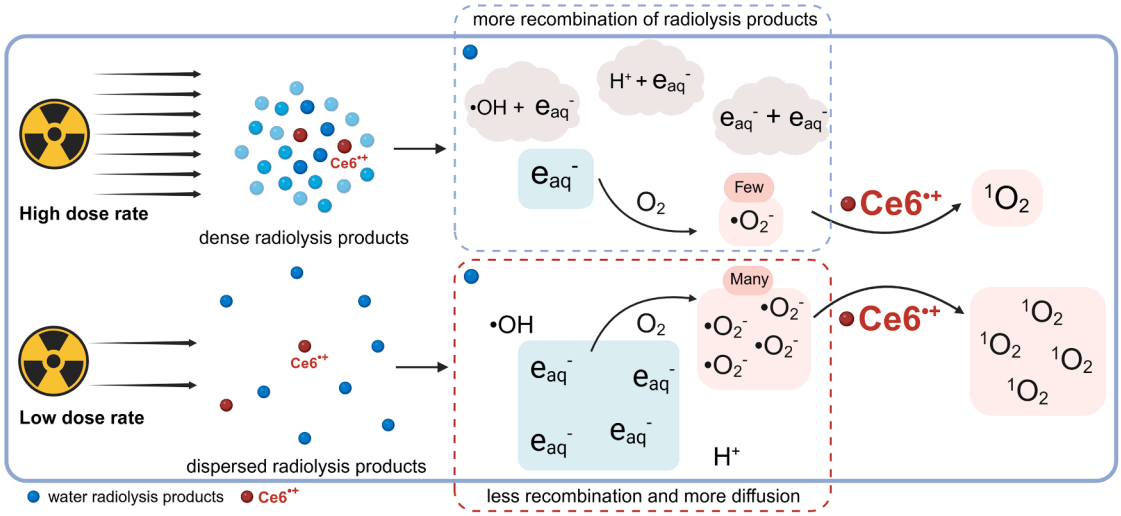

Scheme 1. Schematic illustration of the proposed mechanism for $^1O_2$ generation by Ce6 under high- and low-dose-rate ionizing radiation exposure

The yield of e_{aq}^- decreases with increasing dose rate, likely because e_{aq}^- are involved in numerous radiolysis processes, and at higher dose rates, the denser distribution of radiolysis products increases the chance of radical-radical recombination.[46] Of particular interest is their interaction with O_2 molecules, which leads to the formation of $\cdot O_2^-$, a species that was found to generate $^1O_2$ through a redox reaction.[47] Interestingly, our experiments using SOD to quench $\cdot O_2^-$ eliminated the increased production of $^1O_2$ at low dose rate in both the SOSG and the Imd/RNO methods (Figures 3A and 3B). Additionally, the elimination of $^1O_2$ observed at 20 Gy gamma-ray radiation (Figure 3C) further supports the important role of $\cdot O_2^-$ in $^1O_2$ production by Ce6. While the exact mechanism remains unclear, thermodynamic considerations of the redox potential of $\cdot O_2^-$ and the triplet state of Ce6 (^{3}Ce6*) suggest that direct formation of $^1O_2$ via oxidation of $\cdot O_2^-$ by ^{3}Ce6* is unlikely.[47,48]

We can now propose a possible mechanistic pathway for the generation of $^1O_2$ by Ce6 under ionizing radiation conditions, which differs significantly from traditional photosensitization processes. While conventional photosensitization of Ce6 typically proceeds through excitation to its triplet state, our results suggest that high-energy radiation leads to the formation of Ce6 radical cations (Ce6$^{\cdot+}$). These radical cations can subsequently react with $\cdot O_2^-$ to produce $^1O_2$. The possibility of such a pathway is supported by previous studies reporting the existence of radical cations of photosensitizers when exposed to ionizing radiation.[49,50] In addition, this mechanism is similar to the one proposed by Kavarnos and Turro when describing porphyrin photochemistry.[51] These papers suggest that $^1O_2$ formation can occur either through an energy-transfer process (Equation 1) or stepwise electron exchange in polar solvents (Equations 2 and 3). However, in our radiation-induced system, the conventional photosensitization pathways (Equations 1 and 2) are unfavorable, due to the huge energy gap between ionizing radiation and visible light.

$$^3PS^* + {}^3O_2 \rightarrow PS + {}^1O_2, \quad \text{(Equation 1)}$$

$$^3PS^* + {}^3O_2 \rightarrow PS^+ + \cdot O_2^-, \quad \text{(Equation 2)}$$

$$PS^+ + \cdot O_2^- \rightarrow PS + {}^1O_2. \quad \text{(Equation 3)}$$

Instead, we propose that the electron-exchange reaction between Ce6$^{\cdot+}$ and $\cdot O_2^-$ (Equation 3) dominates the $^1O_2$ generation process, as indicated in Scheme 1. According to the literature, porphyrin compounds typically undergo oxidation at potentials around +0.9 to +1.0 V vs. normal hydrogen electrode (NHE) in aqueous media.[52] Given the structural similarities between Ce6 and these porphyrin compounds, the redox potential of Ce6$^{\cdot+}$ can be estimated to be in a similar range. At this potential, the oxidation of $\cdot O_2^-$ to $^1O_2$ (redox potential at least +0.34 V vs. NHE[47]) would be thermodynamically favorable, supporting this proposed mechanism. Furthermore, the radiolysis of water provides a direct source of $\cdot O_2^-$ that can react with Ce6$^{\cdot+}$, thereby contributing to the generation of $^1O_2$.[53–56]

The enhanced $^1O_2$ generation observed specifically at a very low dose rate suggests a kinetically driven process. At very low dose rates, the extended time between ionization events gives e_{aq}^- more opportunity to react with O_2, favoring the formation of $\cdot O_2^-$ over recombination with other radicals. This increased availability of $\cdot O_2^-$ enhances the interaction with Ce6$^{\cdot+}$. At higher dose rates, a higher dose was required to achieve the same level of $^1O_2$ production, likely because the increased density of radical formation promoted rapid radical-radical recombination, reducing the efficiency of $\cdot O_2^-$ formation and its subsequent reaction with Ce6$^{\cdot+}$. The enhanced $^1O_2$ production observed under gamma-ray radiation compared to X-rays at similar doses may arise from differences in photon energy and their associated linear energy transfer (LET)

characteristics. Gamma rays, with higher initial energy and lower LET, produce more spatially dispersed radicals during water radiolysis, potentially reducing inter-track radical interactions.[57] However, our comparison between only two photon energies cannot conclusively identify LET as the primary driver of enhanced $^1O_2$ generation. Future studies using particle beams with controlled energies could better identify the roles of energy and LET in photosensitizer activation.

From a practical perspective, when considering PSs as radiosensitizers, their biological effects under ionizing radiation arise from a complex interplay of reactive species, not only $^1O_2$ but also ·OH and even PS-derived radicals. Although our experiments confirmed that ·OH is not involved in $^1O_2$ generation by Ce6, we further examined ·OH formation under ionizing radiation in the presence of Ce6 using the aminophenyl fluorescein (APF) probe. As shown in Figure S8, Ce6 enhanced $^1O_2$ production, whereas no increase in ·OH was detected using the APF probe. The APF fluorescence signal with Ce6 was even slightly reduced compared to using APF alone, which may be explained by the ability of Ce6 to scavenge ·OH as mentioned in some studies.[58] These results demonstrate the important role of $^1O_2$ when applying Ce6 as a radiosensitizer. Compared with ·OH or $\cdot O_2^-$, $^1O_2$ remains the most biologically impactful species, as it oxidizes unsaturated lipids, proteins, and nucleic acids and has a relatively long diffusion range.[55,59,60] In addition, studies have found that PS-derived radical cations ($PS^{\cdot+}$) can directly oxidize DNA bases, notably attacking guanine residues and inducing strand lesions,[61] but these effects are local and further restricted by the subcellular distribution of most PSs to mitochondria, lysosomes, and the endoplasmic reticulum rather than the nucleus.[62,63] These findings indicate that while the overall biological effects of PS-mediated radiosensitization arise from the combined actions of multiple ROS and PS radicals, $^1O_2$ still remains the dominant and most biologically significant species. This work focuses on elucidating the generation of $^1O_2$ and its interplay with $\cdot O_2^-$, offering mechanistic insights that may guide future investigations of PS-driven ROS networks. While low-dose-rate modalities such as brachytherapy or radionuclide therapy might enhance $^1O_2$ production, careful consideration and further investigation are required owing to the complexity of intracellular antioxidant defenses, the availability of $\cdot O_2^-$, and dose-rate-dependent alterations in cellular responses.

To conclude, in this study, we systematically investigated the interaction of Ce6 with ionizing radiation, first examining the effects of different photon energies and then exploring the impact of dose rates. Notably, enhanced $^1O_2$ generation was observed at very low dose rates (0.005 Gy/min). Through scavenging experiments, we identified $\cdot O_2^-$ as a possible key intermediate in $^1O_2$ formation. Our mechanistic investigation suggests that, unlike traditional photosensitization where triplet states dominate, Ce6 activation by ionizing radiation proceeds primarily through free radical reactions, with $Ce6^{\cdot+}$ interacting with radiation-induced $\cdot O_2^-$ to generate $^1O_2$. The enhanced efficiency at low dose rates and high-energy radiation indicates that radical lifetime and spatial distribution play crucial roles in this process. The involvement of $\cdot O_2^-$ in this mechanism suggests that the therapeutic efficacy of combined photosensitizer-radiation treatment may be influenced by the oxidative stress status of cancer cells, especially those with elevated ROS levels and reduced SOD activity.[64] Our data also suggest that low-dose-rate treatments like brachytherapy and radionuclide therapy may be more effective when combined with PSs, as they maintain continuous ROS generation in cancer cells[65] and enhance the production of $^1O_2$ by Ce6. However, extensive biological studies would need to be performed to confirm whether in a cellular environment the same effects would occur.

A primary limitation of this study lies in the reliance on indirect methods for detection of $^1O_2$. While we employed both SOSG fluorescence and the Imd/RNO bleaching assay, these approaches are inherently less sensitive than direct detection methods and may fail to capture short-lived species. This limitation may partly explain why no detectable $^1O_2$ signal was observed at 5 Gy under higher dose rates of radiation in our experiments, even though photosensitizers at this dose and within this dose-rate range are known to induce cytotoxic effects.[66] Second, although our scavenging experiments strongly suggest the involvement of $\cdot O_2^-$ in $^1O_2$ formation, direct observation of the reaction between $Ce6^{\cdot+}$ and $\cdot O_2^-$ was not achieved due to the technical challenges in detecting these short-lived species during irradiation. Finally, the preferential formation of $^1O_2$ through the $\cdot O_2^-$ pathway rather than traditional triplet-state mechanisms requires further investigation. Specifically, computational simulations and experimental studies should quantify how efficiently superoxide is formed under different dose rates and radiation qualities.

METHODS

Materials

Ce6 was purchased from Santa Cruz Biotechnology (#SC-263067, purity >96%). SOSG and RNO were purchased from Thermo Fisher Scientific. L-Histidine, SOD, and APF were purchased from Merck Sigma. Ethanol was purchased from Sigma-Aldrich. MQ water used in these experiments was prepared with an in-house Milli-Q system from Merck Millipore.

Radiation source

The X-rays were generated by the X-ray source, a Philips MCN 321 with variable-energy X-ray tube. A ^{60}Co source (GC220, Nordion) was used to generate gamma-ray radiation. The dose rates of ^{60}Co were calculated using Fricke dosimetry corrected for the 2,778-day half-life of cobalt-60.

X-ray and gamma-ray irradiation

For the X-ray irradiation experiments, the samples were positioned on a horizontal platform, located at a specified distance from the X-ray tube. To achieve various dose rates necessary for the experiment, adjustments were made to the ratio of voltage and current. The gamma-ray irradiation was performed at a dose rate of 9.1 Gy/min and 6.2 Gy/min by placing samples into the sample chamber of the ^{60}Co source.

ROS measurement

Singlet oxygen ($^1O_2$) formation was confirmed by two established methods. The first method employed the SOSG probe, which exhibits high selectivity for singlet oxygen detection. The second method, developed by Kraljić and El Mohsni,[67] involves

a combination of Imd group and RNO (referred as the Imd/RNO method).

Measurement of $^1O_2$ by the SOSG probe

A 0.5 mM Ce6 stock solution was prepared by suspending Ce6 powder in MQ water and ultrasonicating for 20 min. The stock solution was then diluted to 10 μM with MQ water. Subsequently, 0.25 mL of 10 μM Ce6 was mixed with an equal volume of 10 μM SOSG solution, resulting in a final concentration of 5 μM Ce6 and SOSG. Both the mixtures and control samples (containing SOSG and water only) were then exposed to either X-rays or gamma-rays. After irradiation, the fluorescence of SOSG was measured at an excitation wavelength of 504 nm and an emission wavelength of 524 nm using a Cary Eclipse fluorescence spectrophotometer (Agilent Technologies).

The normalized relative increase in FL intensity was calculated as follows:

$$\text{Relative increased FL intensity} = \frac{\text{FL(Ce6+SOSG at each dose)}}{\text{FL(SOSG alone at each dose)}}, \quad \text{(Equation 4)}$$

$$\text{Normalized relative FL intensity} = \frac{\text{Relative FL(Ce6+SOSG at each dose)}}{\text{Relative FL(Ce6+SOSG at 0 Gy)}}. \quad \text{(Equation 5)}$$

First, the increased FL intensity of the Ce6 groups relative to the control groups was calculated by dividing the FL intensity of the Ce6 groups by the FL intensity of the control groups at the same specific dose. The relative FL intensity obtained from the first step was then normalized by comparing it to the FL intensity at 0 Gy.

Confirmation of $^1O_2$ by the Imd/RNO method

This method involves two main steps. Initially, $^1O_2$ reacts rapidly with the Imd group, leading to its oxidation and the formation of a peroxide intermediate. In our experiment, we used L-histidine, which contains an Imd group, as the reacting molecule. In the subsequent step, this peroxide intermediate reacts with RNO, causing the bleaching of RNO, which can be measured spectrophotometrically at 440 nm. For the assay, solutions of 0.2 mM Ce6, 25 mM L-histidine, and 125 μM RNO were prepared separately in phosphate buffer (PB) (25 mM, pH 7.4). These solutions (Ce6, L-histidine, and RNO) were then mixed in a 96-well plate to achieve a total volume of 200 μL, containing 40 μM Ce6, 10 mM L-histidine, and 50 μM RNO (with or without 0.01% ethanol). The entire plate was then irradiated by X-rays at various dose rates in a dim environment. The absorption of RNO at 440 nm was measured by a microplate scanning spectrophotometer (PowerWave XS, Bio-Tek) before and after the irradiation. For sunlight exposure experiments, the sample preparation was the same as that used in the X-ray irradiation experiments, except that stock solutions of rose bengal (0.1 mM in PB) and Ce6 (0.1 mM in PB) was further diluted to a final concentration of 10 μM.

Assessment of $\cdot O_2^-$ contribution to $^1O_2$ formation using SOD

To investigate the potential role of superoxide anions in the system, the experiments described above were repeated with the addition of SOD. The procedures for both SOSG and Imd/RNO measurements remained identical, except that SOD (1 μg/mL) was added to the samples before irradiation.

Confirmation of ·OH by the APF probe

A 0.5 mM Ce6 stock solution was prepared by suspending Ce6 powder in MQ water and ultrasonicating for 20 min. The stock solution was then diluted to 10 μM with MQ water. Subsequently, 0.5 mL of 10 μM Ce6 was mixed with an equal volume of 5 μM APF solution, resulting in a final concentration of 5 μM Ce6 and 2.5 μM APF. Both the mixtures and control samples (containing APF and water only) were then exposed to X-rays. After irradiation, the fluorescence of APF was measured at an excitation wavelength of 490 nm and an emission wavelength of 515 nm using a Cary Eclipse fluorescence spectrophotometer (Agilent Technologies).

Data analysis

Data with error bars are presented as mean ± SD. Statistical analyses were performed using either one-way or two-way ANOVA as appropriate. GraphPad Prism software (v.8.00) was used for statistical analysis and data visualization. $p < 0.05$ was considered statistically significant.

RESOURCE AVAILABILITY

Lead contact

Requests for further information and resources should be directed to and will be fulfilled by the lead contact, Antonia G. Denkova (a.g.denkova@tudelft.nl).

Materials availability

This study did not generate new, unique reagents.

Data and code availability

- Data reported in this paper will be shared by the lead contact upon request.
- This paper does not report original code.
- Any additional information required to reanalyze the data reported in this paper is available from the lead contact upon request.

ACKNOWLEDGMENTS

This work is financially supported by the China Scholarship Council (grant no. 202106920019). All schematic illustrations presented in this paper were created with BioRender.com using an academic license (https://BioRender.com/yhtw95a and https://BioRender.com/6zn0hvx).

AUTHOR CONTRIBUTIONS

B.X. performed the experiments, analyzed the data, and drafted the manuscript; J.L. provided discussion on radiation chemistry; and R.E. and A.G.D. provided guidance on the experiments, contributed to theoretical discussions, and revised the manuscript.

DECLARATION OF INTERESTS

The authors declare no competing interests.

DECLARATION OF GENERATIVE AI AND AI-ASSISTED TECHNOLOGIES IN THE WRITING PROCESS

During the preparation of this work, the first author used ChatGPT to enhance the language and readability of this paper. After using this tool, the authors reviewed and edited the content as needed and take full responsibility for the content of the publication.

SUPPLEMENTAL INFORMATION

Supplemental information can be found online at https://doi.org/10.1016/j.xcrp.2025.102976.

Received: June 12, 2025
Revised: September 24, 2025
Accepted: October 30, 2025
Published: November 26, 2025

REFERENCES

1. Barton, M.B., Jacob, S., Shafiq, J., Wong, K., Thompson, S.R., Hanna, T.P., and Delaney, G.P. (2014). Estimating the demand for radiotherapy from the evidence: a review of changes from 2003 to 2012. Radiother. Oncol. *112*, 140–144. https://doi.org/10.1016/j.radonc.2014.03.024.

2. Dash, A., Knapp, F.F.R., Pillai, M.R.A., Dash, A., Knapp, F.F.R., and Pillai, M.R.A. (2013). Targeted Radionuclide Therapy - An Overview. Curr. Radiopharm. *6*, 152–180. https://doi.org/10.2174/18744710113066660023.

3. Baskar, R., Lee, K.A., Yeo, R., and Yeoh, K.W. (2012). Cancer and Radiation Therapy: Current Advances and Future Directions. Int. J. Med. Sci. *9*, 193–199. https://doi.org/10.7150/ijms.3635.

4. Chargari, C., Deutsch, E., Blanchard, P., Gouy, S., Martelli, H., Guérin, F., Dumas, I., Bossi, A., Morice, P., Viswanathan, A.N., and Haie-Meder, C. (2019). Brachytherapy: An overview for clinicians. CA Cancer J. Clin. *69*, 386–401. https://doi.org/10.3322/caac.21578.

5. Berg, K., Luksiene, Z., Moan, J., and Ma, L. (1995). Combined treatment of ionizing radiation and photosensitization by 5-aminolevulinic acid-induced protoporphyrin IX. Radiat. Res. *142*, 340–346. https://doi.org/10.2307/3579143.

6. Adeberg, S., König, L., Bostel, T., Harrabi, S., Welzel, T., Debus, J., and Combs, S.E. (2014). Glioblastoma Recurrence Patterns After Radiation Therapy With Regard to the Subventricular Zone. Int. J. Radiat. Oncol. Biol. Phys. *90*, 886–893. https://doi.org/10.1016/j.ijrobp.2014.07.027.

7. Bartelink, H., Horiot, J.C., Poortmans, P., Struikmans, H., Van den Bogaert, W., Barillot, I., Fourquet, A., Borger, J., Jager, J., Hoogenraad, W., et al. (2001). Recurrence rates after treatment of breast cancer with standard radiotherapy with or without additional radiation. N. Engl. J. Med. *345*, 1378–1387. https://doi.org/10.1056/NEJMoa010874.

8. Wardman, P. (2007). Chemical Radiosensitizers for Use in Radiotherapy. Clin. Oncol. *19*, 397–417. https://doi.org/10.1016/j.clon.2007.03.010.

9. Stupp, R., Mason, W.P., Van Den Bent, M.J., Weller, M., Fisher, B., Taphoorn, M.J.B., Belanger, K., Brandes, A.A., Marosi, C., Bogdahn, U., et al. (2005). Radiotherapy plus Concomitant and Adjuvant Temozolomide for Glioblastoma. N. Engl. J. Med. *352*, 987–996. https://doi.org/10.1056/nejmoa043330.

10. Pepper, N.B., Stummer, W., and Eich, H.T. (2022). The use of radiosensitizing agents in the therapy of glioblastoma multiforme—a comprehensive review. Strahlenther. Onkol. *198*, 507–526. https://doi.org/10.1007/s00066-022-01942-1.

11. Allison, R.R., Downie, G.H., Cuenca, R., Hu, X.H., Childs, C.J., and Sibata, C.H. (2004). Photosensitizers in clinical PDT. Photodiagnosis Photodyn. Ther. *1*, 27–42. https://doi.org/10.1016/S1572-1000(04)00007-9.

12. Schwartz, S., Absolon, K., and Vermund, H. (1955). Hospital Report Porphyrins, X-Rays and Tumors. Univ. Minnesota Med. Bull. *27*, 1–37.

13. Schaffer, M., Schaffer, P.M., Corti, L., Gardiman, M., Sotti, G., Hofstetter, A., Jori, G., and Dühmke, E. (2002). Photofrin as a specific radiosensitizing agent for tumors: studies in comparison to other porphyrins, in an experimental in vivo model. J. Photochem. Photobiol., B *66*, 157–164. https://doi.org/10.1016/S1011-1344(02)00237-3.

14. Schaffer, M., Schaffer, P.M., Vogesser, M., Ertl-Wagner, B., Rauch, J., Oberneder, R., Jori, G., Hofstetter, A., and Dühmke, E. (2002). Application of Photofrin II as a specific radiosensitising agent in patients with bladder cancer—a report of two cases. Photochem. Photobiol. Sci. *1*, 686–689. https://doi.org/10.1039/b203732g.

15. Schaffer, M., Ertl-Wagner, B., Schaffer, P.M., Kulka, U., Jori, G., Wilkowski, R., Hofstetter, A., and Dühmke, E. (2006). Feasibility of Photofrin II as a Radiosensitizing Agent in Solid Tumors – Preliminary Results. Onkologie *29*, 514–519. https://doi.org/10.1159/000095979.

16. Schaffer, P., Batash, R., Ertl-Wagner, B., Hofstetter, A., Asna, N., and Schaffer, M. (2019). Treatment of cervix carcinoma FIGO IIIb with Photofrin II as a radiosensitizer: a case report. Photochem. Photobiol. Sci. *18*, 1275–1279. https://doi.org/10.1039/c8pp00576a.

17. Pignatelli, P., Umme, S., D'Antonio, D.L., Piattelli, A., and Curia, M.C. (2023). Reactive Oxygen Species Produced by 5-Aminolevulinic Acid Photodynamic Therapy in the Treatment of Cancer. Int. J. Mol. Sci. *24*, 8964. https://doi.org/10.3390/ijms24108964.

18. Cozzens, J.W., Lokaitis, B.C., Delfino, K., Hoeft, A., Moore, B.E., Fifer, A.S., Amin, D.V., Espinosa, J.A., Jones, B.A., and Acakpo-Satchivi, L. (2024). A Phase 2 Sensitivity and Selectivity Study of High-Dose 5-Aminolevulinic Acid in Adult Patients Undergoing Resection of a Newly Diagnosed or Recurrent Glioblastoma. Oper. Neurosurg. *29*, 71–79. https://doi.org/10.1227/ons.0000000000001417.

19. Yang, D.M., Cvetkovic, D., Chen, L., and Ma, C.M.C. (2022). Therapeutic effects of in-vivo radiodynamic therapy (RDT) for lung cancer treatment: a combination of 15MV photons and 5-aminolevulinic acid (5-ALA). Biomed. Phys. Eng. Express *8*, 6. https://doi.org/10.1088/2057-1976/ac9b5c.

20. Takahashi, J., Misawa, M., Murakami, M., Mori, T., Nomura, K., and Iwahashi, H. (2013). 5-Aminolevulinic acid enhances cancer radiotherapy in a mouse tumor model. SpringerPlus *2*, 602. https://doi.org/10.1186/2193-1801-2-602.

21. Panetta, J.V., Cvetkovic, D., Chen, X., Chen, L., and Ma, C.M.C. (2020). Radiodynamic therapy using 15-MV radiation combined with 5-aminolevulinic acid and carbamide peroxide for prostate cancer in vivo. Phys. Med. Biol. *65*, 165008. https://doi.org/10.1088/1361-6560/ab9776.

22. Takahashi, J., Nagasawa, S., Doi, M., Takahashi, M., Narita, Y., Yamamoto, J., Ikemoto, M.J., and Iwahashi, H. (2021). In Vivo Study of the Efficacy and Safety of 5-Aminolevulinic Radiodynamic Therapy for Glioblastoma Fractionated Radiotherapy. Int. J. Mol. Sci. *22*, 9762. https://doi.org/10.3390/ijms22189762.

23. Pepper, N.B., Eich, H.T., Müther, M., Oertel, M., Rehn, S., Spille, D.C., and Stummer, W. (2024). ALA-RDT in GBM: protocol of the phase I/II dose escalation trial of radiodynamic therapy with 5-Aminolevulinic acid in patients with recurrent glioblastoma. Radiat. Oncol. *19*, 11. https://doi.org/10.1186/s13014-024-02408-7.

24. Larue, L., Ben Mihoub, A., Youssef, Z., Colombeau, L., Acherar, S., André, J.C., Arnoux, P., Baros, F., Vermandel, M., and Frochot, C. (2018). Using X-rays in photodynamic therapy: an overview. Photochem. Photobiol. Sci. *17*, 1612–1650. https://doi.org/10.1039/c8pp00112j.

25. Takahashi, J., and Misawa, M. (2009). Characterization of reactive oxygen species generated by protoporphyrin IX under X-ray irradiation. Radiat. Phys. Chem. *78*, 889–898. https://doi.org/10.1016/j.radphyschem.2009.06.036.

26. Kitagawa, T., Yamamoto, J., Tanaka, T., Nakano, Y., Akiba, D., Ueta, K., and Nishizawa, S. (2015). 5-Aminolevulinic acid strongly enhances delayed intracellular production of reactive oxygen species (ROS) generated by ionizing irradiation: Quantitative analyses and visualization of intracellular ROS production in glioma cells in vitro. Oncol. Rep. *33*, 583–590. https://doi.org/10.3892/or.2014.3618.

27. Ueta, K., Yamamoto, J., Tanaka, T., Nakano, Y., Kitagawa, T., and Nishizawa, S. (2017). 5-Aminolevulinic acid enhances mitochondrial stress upon ionizing irradiation exposure and increases delayed production of reactive oxygen species and cell death in glioma cells. Int. J. Mol. Med. *39*, 387–398. https://doi.org/10.3892/ijmm.2016.2841.

28. Axelsson, J., Davis, S.C., Gladstone, D.J., and Pogue, B.W. (2011). Cerenkov emission induced by external beam radiation stimulates molecular

fluorescence. Med. Phys. *38*, 4127–4132. https://doi.org/10.1118/1.3592646.

29. Yang, D.M., Cvetkovic, D., Jr, A.E., Chen, L., and Ma, C.M.C. (2023). Tumor Regression with 5-Aminolevulinic Acid (5-ALA)-Mediated Radiodynamic Therapy (RDT) Using Different Megavoltage Energies. Int. J. Radiat. Oncol. Biol. Phys. *117*, e270. https://doi.org/10.1016/j.ijrobp.2023.06.1236.
30. Spinelli, A.E., and Boschi, F. (2021). Photodynamic Therapy Using Cerenkov and Radioluminescence Light. Front. Phys. *9*, 637120. https://doi.org/10.3389/fphy.2021.637120.
31. Miyamoto, S., Martinez, G.R., Medeiros, M.H.G., and Di Mascio, P. (2003). Singlet molecular oxygen generated from lipid hydroperoxides by the russell mechanism: studies using ^{18}O-labeled linoleic acid hydroperoxide and monomol light emission measurements. J. Am. Chem. Soc. *125*, 6172–6179. https://doi.org/10.1021/ja029115.
32. Liu, H., Carter, P.J.H., Laan, A.C., Eelkema, R., and Denkova, A.G. (2019). Singlet Oxygen Sensor Green is not a Suitable Probe for $^1O_2$ in the Presence of Ionizing Radiation. Sci. Rep. *9*, 8393. https://doi.org/10.1038/s41598-019-44880-2.
33. Kim, S., Fujitsuka, M., and Majima, T. (2013). Photochemistry of Singlet Oxygen Sensor Green. J. Phys. Chem. B *117*, 13985–13992. https://doi.org/10.1021/jp406638.
34. Beddok, A., Lahaye, C., Calugaru, V., De Marzi, L., Fouillade, C., Salvador, S., Fontbonne, J.M., Favaudon, V., and Thariat, J. (2022). A Comprehensive Analysis of the Relationship Between Dose Rate and Biological Effects in Preclinical and Clinical Studies, From Brachytherapy to Flattening Filter Free Radiation Therapy and FLASH Irradiation. Int. J. Radiat. Oncol. Biol. Phys. *113*, 985–995. https://doi.org/10.1016/j.ijrobp.2022.02.009.
35. Viswanathan, A.N., Erickson, B.A., Ibbott, G.S., Small, W., Jr., and Eifel, P.J. (2017). The American College of Radiology and the American Brachytherapy Society practice parameter for the performance of low-dose-rate brachytherapy. Brachytherapy *16*, 68–74. https://doi.org/10.1016/j.brachy.2016.06.013.
36. Sharpatyi, V.A., and Kraljić, I. (1978). Determination of singlet oxygen in radiolysis of aerated aqueous solution. Photochem. Photobiol. *28*, 587–590. https://doi.org/10.1111/j.1751-1097.1978.tb06974.x.
37. Kraljić, I., and Trumbore, C.N. (1965). p-Nitrosodimethylaniline as an OH radical scavenger in radiation chemistry. J. Am. Chem. Soc. *87*, 2547–2550. https://doi.org/10.1021/ja01090a004.
38. Jansen, J., Knoll, J., Beyreuther, E., Pawelke, J., Skuza, R., Hanley, R., Brons, S., Pagliari, F., and Seco, J. (2021). Does FLASH deplete oxygen? Experimental evaluation for photons, protons, and carbon ions. Med. Phys. *48*, 3982–3990. https://doi.org/10.1002/mp.14917.
39. Zhang, Q., Xiao, G., Sun, Q., Zeng, J., Wang, L., Chen, L., and Charlie Ma, C.M. (2020). Investigation of the Mechanisms of Radio-Dynamic Therapy. Mathews J. Cancer Sci. *5*, 19. https://doi.org/10.30654/mjcs.10024.
40. Gattuso, H., Monari, A., and Marazzi, M. (2017). Photophysics of chlorin e6: from one- and two-photon absorption to fluorescence and phosphorescence. RSC Adv. *7*, 10992–10999. https://doi.org/10.1039/c6ra28616j.
41. Pimblott, S.M., and LaVerne, J.A. (2007). Production of low-energy electrons by ionizing radiation. Radiat. Phys. Chem. *76*, 1244–1247. https://doi.org/10.1016/j.radphyschem.2007.02.012.
42. Cobut, V., Frongillo, Y., Patau, J., Goulet, T., Fraser, M., and Jay-Gerin, J. (1998). Monte Carlo simulation of fast electron and proton tracks in liquid water-I. Physical and physicochemical aspects. Radiat. Phys. Chem. *51*, 229–244. https://doi.org/10.1016/S0969-806X(97)00096-0.
43. Wang, Z., Pang, Y., and Dlott, D.D. (2007). Hydrogen-Bond Disruption by Vibrational Excitations in Water. J. Phys. Chem. A *111*, 3196–3208. https://doi.org/10.1021/jp069027.
44. Boscolo, D., Scifoni, E., Durante, M., Krämer, M., and Fuss, M.C. (2021). oxygen depletion explain the FLASH effect? A chemical track structure analysis. Radiother. Oncol. *162*, 68–75. https://doi.org/10.1016/j.radonc.2021.06.031.
45. Karle, C., Liew, H., Tessonnier, T., Mein, S., Petersson, K., Schömers, C., Scheloske, S., Brons, S., Cee, R., Major, G., et al. (2025). Oxygen consumption measurements at ultra-high dose rate over a wide LET range. Med. Phys. *52*, 1323–1334. https://doi.org/10.1002/mp.17496.
46. Kusumoto, T., Danvin, A., Mamiya, T., Arnone, A., Chefson, S., Galindo, C., Peaupardin, P., Raffy, Q., Kamiguchi, N., Amano, D., et al. (2024). Dose Rate Effects on Hydrated Electrons, Hydrogen Peroxide, and a OH Radical Molecular Probe Under Clinical Energy Protons. Radiat. Res. *201*, 287–293. https://doi.org/10.1667/RADE-23-00244.1.
47. Sawyer, D.T., and Valentine, J.S. (1981). How super is superoxide? Acc. Chem. Res. *14*, 393–400. https://doi.org/10.1021/ar00072.
48. Baptista, M.S., Cadet, J., Greer, A., and Thomas, A.H. (2021). Photosensitization Reactions of Biomolecules: Definition, Targets and Mechanisms. Photochem. Photobiol. *97*, 1456–1483. https://doi.org/10.1111/php.13470.
49. Imamura, T., Takahashi, M., Tanaka, T., Jin, T., Fujimoto, M., Sawamura, S., and Katayama, M. (1984). Optical and ESR studies for the reaction of molybdenum tetraphenylporphyrns in gamma-ray irradiated 2-methyltetrahydrofuran. Inorg. Chem. *23*, 3752–3755. https://doi.org/10.1021/ic00191.
50. Konishi, S., Hoshino, M., and Imamura, M. (1982). Triplet ESR spectrum of the copper porphyrin cation radical. J. Am. Chem. Soc. *104*, 2057–2059. https://doi.org/10.1021/ja00371a060.
51. Kavarnos, G.J., and Turro, N.J. (1986). Photosensitization by reversible electron transfer: theories, experimental evidence, and examples. Chem. Rev. *86*, 401–449. https://doi.org/10.1021/cr00072a005.
52. Manaia, M.N., and Chiorcea-Paquim, A.M. (2023). Solid state electrochemical behaviour of porphine in aqueous media. J. Electroanal. Chem. *929*, 117123. https://doi.org/10.1016/j.jelechem.2022.117123.
53. Schaap, A.P., Zaklika, K.A., Kaskar, B., and Fung, L.W.M. (1980). Mechanisms of photooxygenation. 2. Formation of 1,2-dioxetanes via 9,10-dicyanoanthracene-sensitized electron-transfer processes. J. Am. Chem. Soc. *102*, 389–391. https://doi.org/10.1021/ja00521a073.
54. Silva, E.F.F., Serpa, C., Da, J.M., Monteiro, J.P., Formosinho, S.o.J., Stochel, G., Urbanska, K., Simões, S., Pereira, M.M., and Arnaut, L.G. (2010). Mechanisms of Singlet-Oxygen and Superoxide-Ion Generation by Porphyrins and Bacteriochlorins and their Implications in Photodynamic Therapy. Chemistry *16*, 9273–9286. https://doi.org/10.1002/chem.201000111.
55. Przygoda, M., Bartusik-Aebisher, D., Dynarowicz, K., Cieślar, G., Kawczyk-Krupka, A., and Aebisher, D. (2023). Cellular Mechanisms of Singlet Oxygen in Photodynamic Therapy. Int. J. Mol. Sci. *24*, 16890. https://doi.org/10.3390/ijms242316890.
56. Pandey, N.K., Xiong, W., Wang, L., Chen, W., Bui, B., Yang, J., Amador, E., Chen, M., Xing, C., Athavale, A.A., et al. (2022). Aggregation-induced emission luminogens for highly effective microwave dynamic therapy. Bioact. Mater. *7*, 112–125. https://doi.org/10.1016/j.bioactmat.2021.05.031.
57. Pimblott, S.M., and LaVerne, J.A. (1994). Diffusion-Kinetic Theories for LET Effects on the Radiolysis of Water. J. Phys. Chem. *98*, 6136–6143. https://doi.org/10.1021/j100075.
58. Yu, J.W., Yoon, S.S., and Yang, R. (2001). Iron Chlorin e6 Scavenges Hydroxyl Radical and Protects Human Endothelial Cells against Hydrogen Peroxide Toxicity. Biol. Pharm. Bull. *24*, 1053–1059. https://doi.org/10.1248/bpb.24.1053.
59. Valenzeno, D.P. (1987). Photomodification of biological membranes with emphasis on singlet oxygen mechanisms. Photochem. Photobiol. *46*, 147–160. https://doi.org/10.1111/j.1751-1097.1987.tb04749.x.
60. Skovsen, E., Snyder, J.W., Lambert, J.D.C., Ogilby, P.R., and Ogilby, P.R. (2005). Lifetime and Diffusion of Singlet Oxygen in a Cell. J. Phys. Chem. B *109*, 8570–8573. https://doi.org/10.1021/jp051163.
61. Enescu, M., Steenkeste, K., Enescu, M., Tfibel, F., Perrée-Fauvet, M., and Fontaine-Aupart, M.-P. (2004). Ultrafast Guanine Oxidation by Photoexcited Cationic Porphyrins Intercalated into DNA. J. Phys. Chem. B *108*, 12215–12221. https://doi.org/10.1021/JP048384.
62. Moan, J., Berg, K., Kvam, E., Western, A., Malik, Z., Rück, A., and Schneckenburger, H. (1989). Intracellular localization of photosensitizers.

In Photosensitizing Compounds: Their Chemistry, Biology and Clinical Use: Ciba Foundation Symposium (Wiley Online Library), pp. 95–111. https://doi.org/10.1002/9780470513842.ch7.

63. Oliveira, C.S., Turchiello, R., Kowaltowski, A.J., Indig, G.L., and Baptista, M.S. (2011). Major determinants of photoinduced cell death: Subcellular localization versus photosensitization efficiency. Free Radic. Biol. Med. *51*, 824–833. https://doi.org/10.1016/j.freeradbiomed.2011.05.023.

64. Tumilaar, S.G., Hardianto, A., Dohi, H., and Kurnia, D. (2024). A Comprehensive Review of Free Radicals, Oxidative Stress, and Antioxidants: Overview, Clinical Applications, Global Perspectives, Future Directions, and Mechanisms of Antioxidant Activity of Flavonoid Compounds. J. Chem. *2024*, 1–21. https://doi.org/10.1155/2024/5594386.

65. Xue, H., Du, L., Li, C., Wang, H., Xue, L., Wang, J., and Jiang, P. (2020). 125I Low Dose Rate Radiation Increases Radiotherapy Sensitivity on Esophageal Cancer Cells via Multiple Mechanisms. Oncol. Rep. *43*, 2028–2044. https://doi.org/10.21203/rs.3.rs-92223/v1.

66. Hosoi, Y., Kawamura, M., Ido, T., Takai, Y., Ishii, K., Nemoto, K., Ono, T., Kimura, S., and Sakamoto, K. (1998). Sensitization of cells to ionizing radiation by chlorine6Na. Radiat. Oncol. Investig. *6*, 151–156. https://doi.org/10.1002/(sici)1520-6823(1998)6:4.

67. Kraljić, I., and El Mohsni, S. (1978). A new method for the detection of singlet oxygen in aqueous solutions. Photochem. Photobiol. *28*, 577–581. https://doi.org/10.1111/j.1751-1097.1978.tb06972.x.